Second-Order Extended Kalman Filter for Extended Object and Group Tracking

Shishan Yang[a], Marcus Baum[a]

[a]*Institute of Computer Science*
University of Göttingen, Germany

arXiv:1604.00219v1 [cs.SY] 1 Apr 2016

Abstract

In this paper, we propose a novel method for estimating an elliptic shape approximation of a moving extended object that gives rise to multiple scattered measurements per frame. For this purpose, we parameterize the elliptic shape with its orientation and the lengths of the semi-axes. We relate an individual measurement with the ellipse parameters by means of a multiplicative noise model and derive a second-order extended Kalman filter for a closed-form recursive measurement update. The benefits of the new method are discussed by means of Monte Carlo simulations for both static and dynamic scenarios.

1. Introduction

Extended object tracking is becoming increasingly important in many application areas such as autonomous driving [22] and maritime surveillance [21]. An extended object is characterized by a varying number of noisy measurements from different spatially distributed sources on the object. In contrast to point target tracking, the objective is to estimate both the location and shape of the target object. Typically, only few measurements are available per frame so that it becomes necessary to systematically fuse measurements from different frames under incorporation of the temporal evaluation of the object.

Many different extended object tracking methods with different properties and application areas have been developed in the past years. For a recent overview of extended object tracking and its applications, we refer to [23]. A main challenge in extended object tracking is that joint tracking and shape estimation is a high-dimensional problem with severe nonlinearities, which requires sophisticated and problem-specific nonlinear estimation techniques.

One of the first approaches is the random matrix approach [28, 29, 17, 16, 18, 20, 19, 24, 26] that models the spatial extent with a Gaussian distribution whose covariance matrix is recursively estimated. For this purpose, the uncertainty of the covariance matrix is represented with an inverse Wishart density.

The random hypersurface (RH) model [1, 4, 3, 13, 12, 11, 10, 14, 13, 15] reduces the extended object tracking problem to a curve fitting problem by means of scaling the shape contours. This idea can be used for basic geometric shapes such as ellipses but also for general star-convex shapes and three-dimensional objects. In the RH approach the shape parameters are estimated using Gaussian estimators such as the Unscented Kalman Filter (UKF) [27]. Of course, in general, the increased flexibility comes at the cost of more complex algorithms.

Monte Carlo methods for extended object and group tracking problems are described in [35, 37, 36, 32].

The objective of this paper is to develop a *Gaussian* state estimator, i.e., nonlinear Kalman filter, for the measurement model of the *random matrix approach* [20].

Email addresses: shishan.yang@cs.uni-goettingen.de (Shishan Yang), marcus.baum@cs.uni-goettingen.de (Marcus Baum)

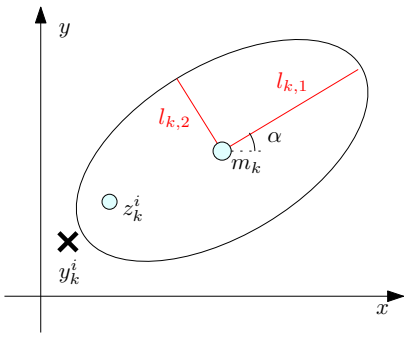

Figure 1: Measurement model and ellipse parameterization. The i-th measurement source at time t is z_k^i. Corresponding measurement y_k^i is z_k^i added with measurement noise. The object shape is modeled using state vector $x_k = [m_k^T, \alpha_k, l_k^T]^T$, where m_k is the center, α_k indicates the object orientation, and $l_k = [l_{k,1}, l_{k,2}]^T$ describes the size of the extended object.

First, we define a suitable parameterization of an arbitrary-oriented ellipse using the orientation and the length of the semi-axes. Second, we form a (polynomial) measurement function that relates a measurement to the state vector (including kinematic and shape parameters). For this purpose, we follow the idea of our previous work [2], where a multiplicative noise is used to model the spatial extent of an extended object. In order to perform a closed-form measurement update based on the derived measurement equation, we derive a second-order extended Kalman filter (SOEKF) [38].

In contrast to the random matrix approach, the proposed method maintains the mean and joint covariance of the kinematic parameters, orientation, and lengths of the semi-axes. Hence, from a modeling point of view, the process model for the shape can directly work with the individual shape parameters. Due to the standard Gaussian representation of the state vector our approach is easy to embed into multi-extended object tracking algorithms.

2. Extended Object Model

This section introduces the state vector, measurement model, and process model used in work for tracking a single extended object.

2.1. State Vector and Shape Parametrization

The state vector

$$x_k = \left[m_k^T, p_k^T, r_k^T\right]^T \tag{1}$$

consists of both kinematic parameters, i.e., center $m_k \in \mathbb{R}^2$ and possibly further quantities $r_k \in \mathbb{R}^{n_r}$ (e.g., velocity), and shape parameters $p_k \in \mathbb{R}^{n_p}$. We propose a parameterization of an ellipse shape according to

$$p_k = \left[\alpha_k, l_{k,1}, l_{k,2}\right]^T \in \mathbb{R}^3 \tag{2}$$

where

- $\alpha_k \in [0, \frac{\pi}{2}]$ specifies the orientation at time step k, and
- $l_{k,1} \in \mathbb{R}^+$ and $l_{k,2} \in \mathbb{R}^+$ specify the lengths of semi-axis.

Note that this is probably the most obvious and intuitive parameterization of an ellipse. For example, it has also been used in [25] for a different measurement model. Besides ellipse, this parameterization could be employed for other perpendicular axis symmetric shapes, e.g., rectangles.

2.2. Measurement Model

At each time k, the extended object gives rise to n_k (independent) two-dimensional measurements

$$\mathcal{Y}_k = \{y_k^i\}_{i=1}^{n_k} \ .$$

Following the idea of [2] of modeling the measurement spread as multiplicative noise and using our parameterization (2), we can form the measurement equation

$$\begin{aligned} y_k^i &= m_k + h_{k,1}^i \cdot l_{k,1} \cdot \begin{bmatrix} \cos\alpha_k \\ \sin\alpha_k \end{bmatrix} + h_{k,2}^i \cdot l_{k,2} \cdot \begin{bmatrix} -\sin\alpha_k \\ \cos\alpha_k \end{bmatrix} + v_k^i \\ &=: h(x_k, v_k^i, h_k^i) \end{aligned} \tag{3}$$

with

- zero-mean multiplicative (Gaussian) noise $h_k^i = \left[h_{k,1}^i, h_{k,2}^i\right]^T \in \mathbb{R}^2$ with covariance $\mathrm{diag}(c_1, c_2)$, where c_1 and c_2 are constant factors that specify the spread of the measurements on the object, and
- additive measurement noise v_k^i with covariance $\mathbf{Q}_k^i$.

Intuitively, $h_{k,1}^i$ and $h_{k,2}^i$ in (3) randomly scale the semi-axis of the ellipse.

A noise-free measurement ($v_k^i = \mathbf{0}$) is also called "measurement source", see Fig. 1. As the measurement source is supposed to lie on the ellipse, physical meaningful values of $h_{k,1}^i$ and $h_{k,2}^i$ should lie in $[-1, 1]$, e.g., a uniform distribution on $[-1, 1]$ would be reasonable.

2.3. Process Model

For the sake of simplicity, we focus on linear process models

$$x_{k+1} = \mathbf{A}_k x_k + w_k \tag{4}$$

where

- $\mathbf{A}_k$ is the system matrix, and
- w_k is zero-mean white Gaussian process noise with covariance matrix $\mathbf{P}_k$.

3. Relationship to the Random Matrix Measurement Model

The random matrix approach introduced in [16] employs the likelihood function

$$p(y_k^i | m_k, \mathbf{X}) \sim \mathcal{N}(y_k^i; m_k, c\mathbf{X}_k + \mathbf{Q}_k^i) \tag{5}$$

where

- $\mathbf{X}_k$ is a symmetric positive definite matrix that specifies the elliptic extent,
- Constant scaling $c \in \mathbb{R}$, e.g., to match uniform noise,
- $\mathbf{Q}_k^i$ is the measurement noise covariance.

Actually, the corresponding likelihood function of measurement equation (3) coincides with (5) if h_k^i is Gaussian distributed. Only the parameterization of the ellipse differs. In order to show that, we first note that any covariance matrix $\mathbf{X}_k$ can be written as

$$\mathbf{X}_k = \mathbf{R}_k \mathbf{D}_k \mathbf{R}_k^T \tag{6}$$

with

$$\mathbf{R}_k = \begin{bmatrix} \cos\alpha_k & -\sin\alpha_k \\ \sin\alpha_k & \cos\alpha_k \end{bmatrix} \tag{7}$$

$$\mathbf{D}_k = \begin{bmatrix} (l_{k,1})^2 & 0 \\ 0 & (l_{k,2})^2 \end{bmatrix} \ . \tag{8}$$

In this manner, (3) can be written as

$$y_k^i = m_k + \mathbf{R}_k \sqrt{\mathbf{D}_k} \cdot h_k^i + v_k^i \ , \tag{9}$$

which is the standard generative equation for sampling from a multivariate Gaussian (for $v_k^i = \mathbf{0}$ and $c = 1$).

4. Second-Order Extended Kalman Filter

In this section, we derive a second-order Kalman filter (SOEKF) for recursively estimating the kinematic and shape parameters of an extended object based on the models introduced in the previous section. As we have to deal with multiple measurements per time step, we will process the measurements sequentially. For this purpose, let $\hat{x}_k^i$ and $\mathbf{C}_k^i$ denote the mean and covariance of the estimate having incorporated all measurements up to the i-th measurement of time k. According to this, notation $\hat{x}_k^0$ and $\mathbf{C}_k^0$ represent the prediction for time k, having not yet incorporated a measurement from time k.

4.1. Measurement Update

As shown in our previous work [2] for (axis-aligned) ellipses, the optimal *linear* estimator is not feasible for the multiplicative noise model (3) as there are not "enough" correlations between the measurement and state vector. Hence, we create a *quadratic* estimator by forming a pseudo-measurement from the original measurement and the 2-fold Kronecker product

$$(y_k^i)^{[2]} = \begin{bmatrix} (y_{k,1}^i)^2 \\ (y_{k,2}^i)^2 \\ y_{k,1}^i \cdot y_{k,2}^i \end{bmatrix} \ .$$

Furthermore, we shift the (estimated) center $\hat{m}_k^{i-1}$ of the object to the origin in order to avoid numerical problems due to the squared equation. It is important to note that all these reformulations do not change the original likelihood function. However, when using the Kalman filter update equations, an improvement can be achieved as the squared measurements are incorporated. This concept is widely-known and frequently used in literature, see for example [8, 6, 2, 31, 30, 40]. All told, the final measurement equation becomes

$$\underbrace{\begin{bmatrix} y_k^i - \hat{m}_k^{i-1} \\ (y_k^i - \hat{m}_k^{i-1})^{[2]} \end{bmatrix}}_{:=z_k^i} = \underbrace{\begin{bmatrix} h(x_k, v_k^i, h_k^i) - \hat{m}_k^{i-1} \\ (h(x_k, v_k^i, h_k^i) - \hat{m}_k^{i-1})^{[2]} \end{bmatrix}}_{:=g(x_k, v_k^i, h_k^i)} \ . \tag{10}$$

Based on (10) the Kalman filter update becomes

$$\hat{x}_k^i = \hat{x}_k^{i-1} + \mathbf{M}_k^i (\mathbf{S}_k^i)^{-1} (z_k^i - \hat{z}_k^i) \tag{11}$$

$$\mathbf{C}_k^i = \mathbf{C}_k^{i-1} - \mathbf{M}_k^i (\mathbf{S}_k^i)^{-1} (\mathbf{M}_k^i)^T \ , \tag{12}$$

with

$$\mathbf{M}_k^i = \mathrm{Cov}[z_k^i, x_k \mid \mathcal{Z}_k^{i-1}] \tag{13}$$

$$\mathbf{S}_k^i = \mathrm{Cov}[z_k^i, z_k^i \mid \mathcal{Z}_k^{i-1}] \tag{14}$$

$$\hat{z}_k^i = \mathrm{E}[z_k^i \mid \mathcal{Z}_k^{i-1}] \tag{15}$$

It turned out that a first-order Taylor series approximation of (10) is not precise enough to capture all nonlinearities. Hence, we propose a second-order Taylor series approximation [38]. If we define the augmented state vector $\gamma_k = \left[x_k^T, (v_k^i)^T, (h_k^i)^T\right]^T$ with $\hat{\gamma}_k^i = \left[(\hat{x}_k^i)^T, 0, 0, 0, 0\right]^T$ and covariance $\mathbf{\Gamma}_k^{i-1} = \mathrm{diag}(\mathbf{C}_k^{i-1}, \mathbf{Q}_k^i, c_1, c_2)$, we obtain [38]

$$\begin{aligned}
\mathrm{E}[z_{k,l}^i \mid \mathcal{Z}_k^{i-1}] &= g_l(\hat{\gamma}_k^i) + \frac{1}{2}\mathrm{Tr}(\mathbf{H}_{k,l}^i \mathbf{\Gamma}_k^i) \\
\mathrm{Cov}[z_{k,l}^i, z_{k,r}^i \mid \mathcal{Z}_k^{i-1}] &= \mathbf{J}_{k,l}^i \mathbf{\Gamma}_k^i (\mathbf{J}_{k,r}^i)^T \\
&\quad + \frac{1}{2}\mathrm{Tr}(\mathbf{H}_{k,l}^i \mathbf{\Gamma}_k^i \mathbf{H}_{k,r}^i \mathbf{\Gamma}_k^i) \\
\mathrm{Cov}[z_k^i, \gamma_k \mid \mathcal{Z}_k^{i-1}] &= \mathbf{\Gamma}_k^i (\mathbf{J}_k^i)^T
\end{aligned}$$

where

- $\mathbf{J}_k^i$ is the Jacobian matrix of g evaluated at $\hat{\gamma}_k^i$. $\mathbf{J}_{k,l}^i$ denotes the l-th row of $\mathbf{J}_k^i$,
- $\mathbf{H}_{k,l}^i$ is the Hessian matrix of the l-th component function of g evaluated at $\hat{\gamma}_k^i$

The Jacobian and Hessians are given in the Appendix. We note that an essential modification of the Jacobian and Hessians is necessary: As the means of $h_{k,1}^i$ and $h_{k,2}^i$ are 0, significant parts of Jacobian and Hessians at $\hat{\gamma}_k^i$ are zero as well. Hence, we substitute $(h_{k,1}^i)^2$ and $(h_{k,2}^i)^2$ in the Jacobian and Hessians by $\mathrm{E}[(h_{k,1}^i)^2] = c_1$ and $\mathrm{E}[(h_{k,2}^i)^2] = c_2$. Without this modifications, the shape parameters do not change in a measurement update.

4.2. Time Update

As the process model is linear and the time update can be performed with the standard Kalman filtering equations.

5. Evaluation

In this section, we first briefly discuss the current approaches used for extend object tracking and suggest a new metric based on a Wasserstein/Optimal Sub-Pattern Assignment (OSPA) distance [39] construction. Then, we evaluate our method for tracking elliptical and rectangular objects in static and dynamic scenarios using suggested metric. In both simulations, we compare our proposed SOEKF estimator with Monte Carlo estimator.

For extended object tracking, the state vector normally includes kinematic and shape parameters [28]. As these quantities are not at the same order of magnitude and different shape parameters can specify the same shape, the overall Root Mean Squared Error (RMSE) of the estimated state would be misleading. This problem can be by-passed by decoupling state properties and calculate their RMSEs separately [1, 18]. Decoupled RMSE gives a more detailed insight for the performance in a certain aspect. To combine object shape, size, and orientation, a similarity measure called Intersection-over-Union (IoU) [25], which is also known as Jaccard index, is widely used in the evaluation of many computer vision tasks, such as image segmentation [9, 7], object detection [41, 34] and tracking [33, 5]. Given two shapes, IoU is the intersected area divided by their union area. Using IoU to evaluate extended object tracking methods still has two major drawbacks. Firstly, IoU is extremely difficult to calculate for non-axis aligned objects as the intersection and union areas are normally irregular shapes (see Fig. 2). In computer vision, IoU is typically calculated either for regular axis-aligned objects or approximated using the number of intersected pixels divided by the number of pixels on the union area. Secondly, even if we could approximate the area of intersection and union by sampling [25], IoU score could not distinguish two estimates when neither of them intersect with ground truth.

Based on the discussion above, we suggest a miss-distance for extended object tracking evaluation based on the Wasserstein/OSPA distance. Rectangular and elliptical objects have two axes of symmetry that intersect the ellipse contour at four points. These four points capture differences in position,

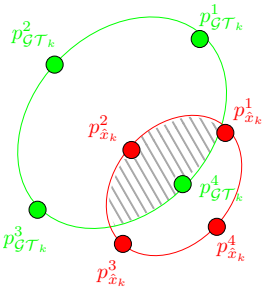

Figure 2: An illustration for the points we selected for evaluation. The red ellipse is estimation $\hat{x}_k$ and the green ellipse indicates ground truth $\mathcal{GT}_k$ in time step k.

shape, size, and orientation, hence, uniquely determine a rectangle or ellipse. We select aforementioned four points from the ground truth ($\mathcal{GT}_k$) and the estimate $\hat{x}_k$ in time step k. This gives two sets of four points (see Fig. 2), $\mathbb{S}_{\mathcal{GT}_k} = \{p^1_{\mathcal{GT}_k}, p^2_{\mathcal{GT}_k}, p^3_{\mathcal{GT}_k}, p^4_{\mathcal{GT}_k}\}$ and $\mathbb{S}_{\hat{x}_k} = \{p^1_{\hat{x}_k}, p^2_{\hat{x}_k}, p^3_{\hat{x}_k}, p^4_{\hat{x}_k}\}$, whose distance can be calculated with the Wasserstein/OSPA according to

$$\mathbf{d}(\hat{x}_k, \mathcal{GT}_k) = \frac{1}{4} \min_{\pi \in \Pi} \sum_{i}^{4} \parallel p^i_{\mathcal{GT}_k} - p^{\pi(i)}_{\hat{x}_k} \parallel^2 \ , \tag{16}$$

where Π is all permutations of the set $\{1, 2, 3, 4\}$. For perfectly aligned estimate and ground truth, $\mathbf{d}$ is 0, i.e., no estimation error. It it obvious that $\mathbf{d}$ satisfies the identity, symmetry, and triangle inequality that a metric requires. Besides, $\mathbf{d}$ could also compare two estimates even when neither of them intersect with the ground truth.

5.1. Stationary Ellipse

As we derived a SOEKF for closed-form measurement update in Section 4, we would like to evaluate its performance compared to Monte Carlo sampling. In order to focus on measurement update, we first consider a stationary object.

The ground truth ellipse lies at $\tilde{m}_k = [1000, 1000]$, 30 ° counter-clockwise rotated from x-axis, i.e., $\tilde{\alpha}_k = \frac{\pi}{6}$, and the length is $\tilde{l}_k = [2, 1]^T$, for all k. As described in our previous work [2], h^i_k lies on the interval of $[-1, 1]$. To ensure most measurement sources lying on the object extent, multiplicative noise h^i_k follows Gaussian distribution $\mathcal{N}(h^i_k - \mathbf{0}_2, \frac{1}{4}\mathbf{I}_2)$ [18].

We test our approach under three scenarios: no measurement noise ($\mathbf{Q}^i_k = \mathbf{0}_2$), medium measurement noise ($\mathbf{Q}^i_k = \mathbf{I}_2$), and high measurement noise ($\mathbf{Q}^i_k = 4\mathbf{I}_2$). The prior is given by a Gaussian distribution with $9\mathbf{I}$ as covariance of center, $\frac{1}{9}$ as variance of orientation, and $\mathbf{I}_2$ as covariance matrix of lengths.

The measurements, example estimates and mean error for the described simulations are shown in Fig. 3. We can see that proposed SOEKF estimator is slightly worse than Monte Carlo sampling when there is no measurement noise. However, it coincides with Monte Carlo under medium and high measurement noise. The simulations show that the SOEKF gives pretty good approximations for the moments in (11), even though the degree of the measurement equation is much higher than two.

5.2. Rectangle with NCV

In the following, we evaluated our method for tracking a rectangular object follows a Nearly Constant Velocity (NCV) model.

The object initially lies at the origin, the width of the object is $2m$ and length is $4m$, i.e., $\tilde{l}_k = [1, 2]^T$ for all k. The object orientation is aligned with its velocity. For the first 30 and last 40 time steps, the object moves along x axes and the speed is $1.5m$ per time step. In the between, its velocity is $[1.5, 1.5]^T$. The number of measurements in each time step is drawn from a Poisson distribution with mean of 7. The measurement sources are uniformly distributed on the extent of

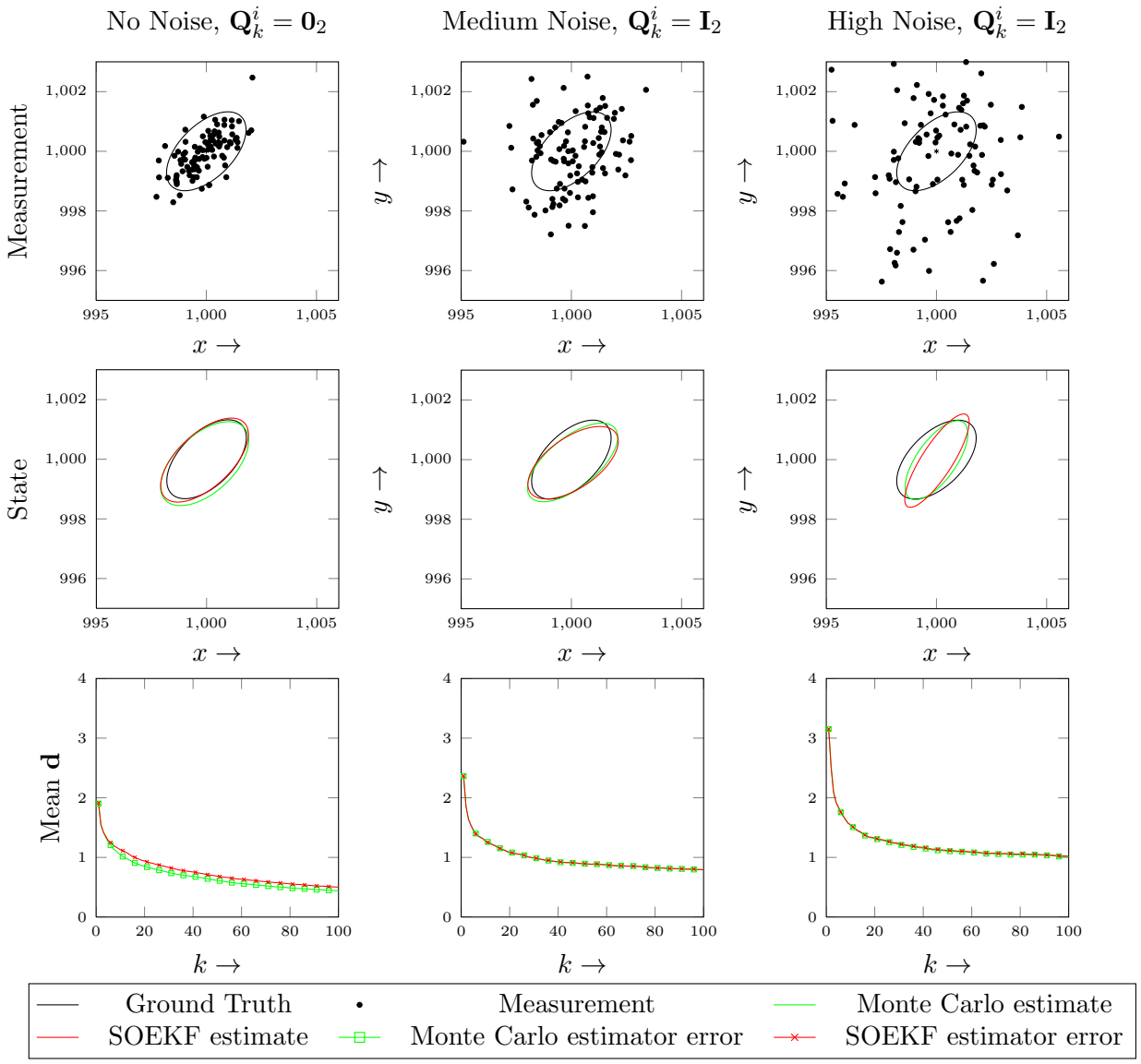

Figure 3: Simulation on static ellipse. The first row figures show the ground truth and measurements. The second row give example estimates after 100 measurements update. The last row plot mean $\mathbf{d}$ for 100 runs.

the object, which results in $h_k^i \sim \mathcal{U}(h_k^i - \mathbf{0}_2, \frac{1}{3}\mathbf{I}_2)$. The measurement noise is zero-mean Gaussian distributed with covariance of $\frac{1}{3}\mathbf{I}_2$. The initial guess are $m_0 = [0.6, 0.6]^T$ with covariance of $\frac{1}{2}\mathbf{I}_2$, $\alpha_0 = \frac{\pi}{3}$ with variance of 0.76, $l_0 = [1.5, 2.5]$ with covariance of $\frac{1}{5}\mathbf{I}_2$, and velocity $[1, 0]^T$ with covariance matrix $\mathbf{I}_2$.

The ground truth and an example estimation result is depicted in Fig. 4 for every third time step. Consistent with the results from the static case, SOEKF estimations overlap with Monte Carlo estimations after sufficient number of measurements.

All told, the simulations demonstrate that the second-order approximation is very accurate even in the case of high noise.

6. Conclusion and Future Work

Simultaneous tracking and shape estimation based on independent noisy point measurements is a challenging nonlinear estimation problem – even for basic shapes such as ellipses. This work started

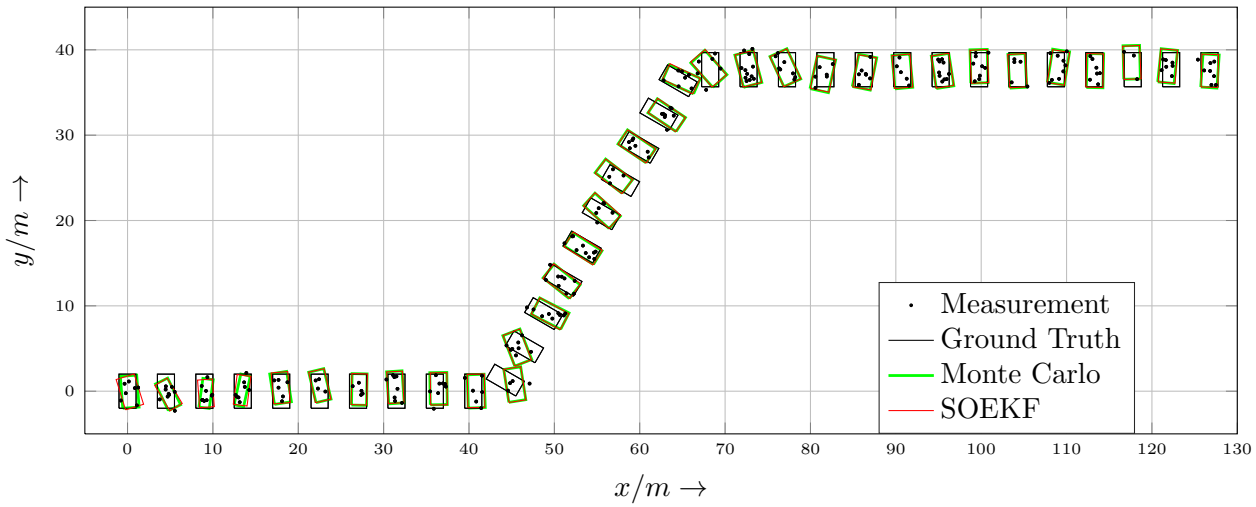

Figure 4: Example tracking result of a rectangle. Ground truth and estimates are plotted for every third time step.

from the idea to develop a standard nonlinear Gaussian estimator for estimating an elliptic shape approximation.

It turned out that three steps are required: (i) A measurement function with multiplicative noise must be formulated. (ii) The measurement equation must be squared; otherwise there are not enough correlations between the measurements and shape parameters. (iii) A first-order Taylor series expansion of the quadratic measurement equation is not sufficient. However, a second-order Taylor series expansion (SOEKF) pretty much matches the exact moments (but only if we substitute the mean of the squared multiplicative noise).

The final equations of the SOEKF are still tractable and rather compact. However, we believe that significant simplifications are possible, e.g., if the kinematic and shape parameters are assumed to be independent.

Appendix A. Jacobian and Hessian matrices

This Appendix gives the Jacobian and Hessian matrix for our SOEKF estimator in Fig. A.5. For compactness, we

- suppress the time index k, measurement index i, and
- omit the kinematic parameters r_k as they do not appear in the measurement equation
- do not differentiate the spread of multiplicative error, i.e., $c_1 = c_2 = c$.

References

[1] M. Baum, "Student Research Highlight: Simultaneous Tracking and Shape Estimation of Extended Targets," *IEEE Aerospace and Electronic Systems Magazine*, vol. 27, no. 7, pp. 42–44, July 2012.

[2] M. Baum, F. Faion, and U. D. Hanebeck, "Modeling the Target Extent with Multiplicative Noise," in *Proceedings of the 15th International Conference on Information Fusion (Fusion 2012)*, Singapore, Jul. 2012.

[3] M. Baum and U. D. Hanebeck, "Extended Object Tracking Based on Set-Theoretic and Stochastic Fusion," *IEEE Transactions on Aerospace and Electronic Systems*, vol. 48, no. 4, pp. 3103–3115, Oct. 2012.

[4] ——, "Extended Object Tracking with Random Hypersurface Models," *IEEE Transactions on Aerospace and Electronic Systems*, vol. 50, pp. 149–159, Jan. 2014.

[5] S. Breuers, S. Yang, M. Mathias, and B. Leibe, "Exploring bounding box context for multi-object tracker fusion," in *IEEE Winter Conference on Applications of Computer Vision (WACV 2016)*, New York, USA, Mar. 2016.

$$
\mathbf{J}_{\cdot}^{\cdot} = \begin{pmatrix}
1 & 0 & 0 & 0 & 0 & l_1 \cos\alpha & -l_2 \sin\alpha & 1 & 0 \\
0 & 1 & 0 & 0 & 0 & l_1 \sin\alpha & l_2 \cos\alpha & 0 & 1 \\
0 & 0 & -c \sin 2\alpha \left({l_1}^2 - {l_2}^2\right) & 2\, l_1\, c \cos^2\alpha & 2\, l_2\, c \sin^2\alpha & 0 & 0 & 0 & 0 \\
0 & 0 & c \sin 2\alpha \left({l_1}^2 - {l_2}^2\right) & 2\, l_1\, c \sin^2\alpha & 2\, l_2\, c \cos^2\alpha & 0 & 0 & 0 & 0 \\
0 & 0 & c \cos 2\alpha \left({l_1}^2 - {l_2}^2\right) & l_1\, c \sin 2\alpha & -l_2\, c \sin 2\alpha & 0 & 0 & 0 & 0
\end{pmatrix}
$$

$$
\mathbf{H}_{\cdot,1}^{\cdot} = \begin{pmatrix}
0 & 0 & 0 & 0 & 0 & 0 & 0 & 0 & 0 \\
0 & 0 & 0 & 0 & 0 & 0 & 0 & 0 & 0 \\
0 & 0 & 0 & 0 & 0 & -l_1 \sin\alpha & -l_2 \cos\alpha & 0 & 0 \\
0 & 0 & 0 & 0 & 0 & \cos\alpha & 0 & 0 & 0 \\
0 & 0 & 0 & 0 & 0 & 0 & -\sin\alpha & 0 & 0 \\
0 & 0 & -l_1 \sin\alpha & \cos\alpha & 0 & 0 & 0 & 0 & 0 \\
0 & 0 & -l_2 \cos\alpha & 0 & -\sin\alpha & 0 & 0 & 0 & 0 \\
0 & 0 & 0 & 0 & 0 & 0 & 0 & 0 & 0 \\
0 & 0 & 0 & 0 & 0 & 0 & 0 & 0 & 0
\end{pmatrix}
$$

$$
\mathbf{H}_{\cdot,2}^{\cdot} = \begin{pmatrix}
0 & 0 & 0 & 0 & 0 & 0 & 0 & 0 & 0 \\
0 & 0 & 0 & 0 & 0 & 0 & 0 & 0 & 0 \\
0 & 0 & 0 & 0 & 0 & l_1 \cos\alpha & -l_2 \sin\alpha & 0 & 0 \\
0 & 0 & 0 & 0 & 0 & \sin\alpha & 0 & 0 & 0 \\
0 & 0 & 0 & 0 & 0 & 0 & \cos\alpha & 0 & 0 \\
0 & 0 & l_1 \cos\alpha & \sin\alpha & 0 & 0 & 0 & 0 & 0 \\
0 & 0 & -l_2 \sin\alpha & 0 & \cos\alpha & 0 & 0 & 0 & 0 \\
0 & 0 & 0 & 0 & 0 & 0 & 0 & 0 & 0 \\
0 & 0 & 0 & 0 & 0 & 0 & 0 & 0 & 0
\end{pmatrix}
$$

$$
\mathbf{H}_{\cdot,3}^{\cdot} = \begin{pmatrix}
2 & 0 & 0 & 0 & 0 & 2\, l_1 \cos\alpha & -2\, l_2 \sin\alpha & 2 & 0 \\
0 & 0 & 0 & 0 & 0 & 0 & 0 & 0 & 0 \\
0 & 0 & -2\, c \cos 2\alpha \left({l_1}^2 - {l_2}^2\right) & -2\, l_1\, c \sin 2\alpha & 2\, l_2\, c \sin 2\alpha & 0 & 0 & 0 & 0 \\
0 & 0 & -2\, l_1\, c \sin 2\alpha & 2\, c \cos^2\alpha & 0 & 0 & 0 & 0 & 0 \\
0 & 0 & 2\, l_2\, c \sin 2\alpha & 0 & 2\, c \sin^2\alpha & 0 & 0 & 0 & 0 \\
2\, l_1 \cos\alpha & 0 & 0 & 0 & 0 & 2\, {l_1}^2 \cos^2\alpha & -l_1\, l_2 \sin 2\alpha & 2\, l_1 \cos\alpha & 0 \\
-2\, l_2 \sin\alpha & 0 & 0 & 0 & 0 & -l_1\, l_2 \sin 2\alpha & 2\, {l_2}^2 \sin^2\alpha & -2\, l_2 \sin\alpha & 0 \\
2 & 0 & 0 & 0 & 0 & 2\, l_1 \cos\alpha & -2\, l_2 \sin\alpha & 2 & 0 \\
0 & 0 & 0 & 0 & 0 & 0 & 0 & 0 & 0
\end{pmatrix}
$$

$$
\mathbf{H}_{\cdot,4}^{\cdot} = \begin{pmatrix}
0 & 0 & 0 & 0 & 0 & 0 & 0 & 0 & 0 \\
0 & 2 & 0 & 0 & 0 & 2\, l_1 \sin\alpha & 2\, l_2 \cos\alpha & 0 & 2 \\
0 & 0 & 2\, c \cos 2\alpha \left({l_1}^2 - {l_2}^2\right) & 2\, l_1\, c \sin 2\alpha & -2\, l_2\, c \sin 2\alpha & 0 & 0 & 0 & 0 \\
0 & 0 & 2\, l_1\, c \sin 2\alpha & 2\, c \sin^2\alpha & 0 & 0 & 0 & 0 & 0 \\
0 & 0 & -2\, l_2\, c \sin 2\alpha & 0 & 2\, c \cos^2\alpha & 0 & 0 & 0 & 0 \\
0 & 2\, l_1 \sin\alpha & 0 & 0 & 0 & 2\, {l_1}^2 \sin^2\alpha & l_1\, l_2 \sin 2\alpha & 0 & 2\, l_1 \sin\alpha \\
0 & 2\, l_2 \cos\alpha & 0 & 0 & 0 & l_1\, l_2 \sin 2\alpha & 2\, {l_2}^2 \cos^2\alpha & 0 & 2\, l_2 \cos\alpha \\
0 & 0 & 0 & 0 & 0 & 0 & 0 & 0 & 0 \\
0 & 2 & 0 & 0 & 0 & 2\, l_1 \sin\alpha & 2\, l_2 \cos\alpha & 0 & 2
\end{pmatrix}
$$

$$
\mathbf{H}_{\cdot,5}^{\cdot} = \begin{pmatrix}
0 & 1 & 0 & 0 & 0 & l_1 \sin\alpha & l_2 \cos\alpha & 0 & 1 \\
1 & 0 & 0 & 0 & 0 & l_1 \cos\alpha & -l_2 \sin\alpha & 1 & 0 \\
0 & 0 & -2\, c \sin 2\alpha \left({l_1}^2 - {l_2}^2\right) & 2\, l_1\, c \cos 2\alpha & -2\, l_2\, c \cos 2\alpha & 0 & 0 & 0 & 0 \\
0 & 0 & 2\, l_1\, c \cos 2\alpha & c \sin 2\alpha & 0 & 0 & 0 & 0 & 0 \\
0 & 0 & -2\, l_2\, c \cos 2\alpha & 0 & -c \sin 2\alpha & 0 & 0 & 0 & 0 \\
l_1 \sin\alpha & l_1 \cos\alpha & 0 & 0 & 0 & {l_1}^2 \sin 2\alpha & l_1\, l_2 \cos 2\alpha & l_1 \sin\alpha & l_1 \cos\alpha \\
l_2 \cos\alpha & -l_2 \sin\alpha & 0 & 0 & 0 & l_1\, l_2 \cos 2\alpha & -{l_2}^2 \sin 2\alpha & l_2 \cos\alpha & -l_2 \sin\alpha \\
0 & 1 & 0 & 0 & 0 & l_1 \sin\alpha & l_2 \cos\alpha & 0 & 1 \\
1 & 0 & 0 & 0 & 0 & l_1 \cos\alpha & -l_2 \sin\alpha & 1 & 0
\end{pmatrix}
$$

Figure A.5: Jacobian matrix and Hessian matrices for the SOEKF. Note that the Hessian matrices are symmetric.

[6] F. Carravetta, A. Germani, and N. Raimondi, "Polynomial Filtering of Discrete-Time Stochastic Linear Systems with Multiplicative State Noise," *IEEE Transactions on Automatic Control*, vol. 42, no. 8, pp. 1106 –1126, August 1997.

[7] G. Csurka, D. Larlus, and F. Perronnin, "What is a good evaluaton measure for semantic segmentation?" in *In 24th British Machine Vision Conference (BMVC 2013)*, Bristol, Sept. 2013.

[8] A. De Santis, A. Germani, and M. Raimondi, "Optimal Quadratic Filtering of Linear Discrete-time Non-Gaussian Systems," *IEEE Transactions on Automatic Control*, vol. 40, no. 7, pp. 1274 –1278, July 1995.

[9] M. Everingham, S. M. A. Eslami, L. V. Gool, C. K. I. Williams, J. Winn, and A. Zisserman, "The pascal visual object classes challenge: A retrospective," *International Journal of Computer Vision*, vol. 111, no. 1, pp. 98–136, 2015.

[10] F. Faion, M. Baum, and U. D. Hanebeck, "Tracking 3D Shapes in Noisy Point Clouds with Random Hypersurface Models," in *Proceedings of the 15th International Conference on Information Fusion (Fusion 2012)*, Singapore, Jul. 2012.

[11] ——, "Silhouette Measurements for Bayesian Object Tracking in Noisy Point Clouds," in *Proceedings of the 16th International Conference on Information Fusion (Fusion 2013)*, Istanbul, Turkey, Jul. 2013.

[12] ——, "Depth Sensor Calibration by Means of Tracking an Extended Object," in *Proceedings of the 2015 IEEE International Conference on Multisensor Fusion and Information Integration (MFI 2015)*, San Diego, California, USA, Sep. 2015.

[13] F. Faion, A. Zea, M. Baum, and U. D. Hanebeck, "Bayesian Estimation of Line Segments," in *Proceedings of the IEEE ISIF Workshop on Sensor Data Fusion: Trends, Solutions, Applications (SDF 2014)*, Bonn, Germany, Oct. 2014.

[14] ——, "Partial Likelihood for Unbiased Extended Object Tracking," in *Proceedings of the 18th International Conference on Information Fusion (Fusion 2015)*, Washington, USA, Jul. 2015.

[15] F. Faion, A. Zea, J. Steinbring, M. Baum, and U. D. Hanebeckk, "Recursive Bayesian Pose and Shape Estimation of 3D Objects Using Transformed Plane Curves," in *Proceedings of the IEEE ISIF Workshop on Sensor Data Fusion: Trends, Solutions, Applications (SDF 2015)*, Bonn, Germany, Oct. 2015.

[16] M. Feldmann and D. Fränken, "Tracking of Extended Objects and Group Targets using Random Matrices – A New Approach," Cologne,Germany, Jul. 2008.

[17] ——, "Advances on Tracking of Extended Objects and Group Targets using Random Matrices," in *Proceedings of the 12th International Conference on Information Fusion (Fusion 2009)*, Seattle, Washington, Jul. 2009.

[18] M. Feldmann, D. Fränken, and W. Koch, "Tracking of Extended Objects and Group Targets using Random Matrices," *IEEE Transactions on Signal Processing*, vol. 59, no. 4, pp. 1409–1420, 2011.

[19] M. Feldmann and W. Koch, "Road-map Assisted Convoy Track Maintenance using Random Matrices," Cologne, Germany, Jul. 2008, pp. 1–8.

[20] ——, "Comments on "Bayesian Approach to Extended Object and Cluster Tracking using Random Matrices"," *IEEE Transactions on Aerospace and Electronic Systems*, vol. 48, no. 2, pp. 1687 –1693, April 2012.

[21] K. Granström, A. Natale, P. Braca, G. Ludeno, and F. Serafino, "PHD Extended Target Tracking Using an Incoherent X-band Radar: Preliminary Real-World Experimental Results," in *Proceedings of the 17th International Conference on Information Fusion (Fusion 2014)*, Salamanca, Spain, Jul. 2014.

[22] K. Granström, S. Reuter, D. Meissner, and A. Scheel, "A multiple model PHD approach to tracking of cars under an assumed rectangular shape," in *Proceedings of the 17th International Conference on Information Fusion (Fusion 2014)*, Salamanca, Spain, Jul. 2014.

[23] K. Granström and M. Baum, "Extended Object Tracking: Introduction, Overview and Applications," *arXiv preprint*, 2016. [Online]. Available: http://arxiv.org/abs/1212.5882

[24] K. Granström, C. Lundquist, and U. Orguner, "A Gaussian Mixture PHD filter for Extended Target Tracking," in *Proceedings of the 13th International Conference on Information Fusion (Fusion 2010)*, Edinburgh, Scotland, Jul. 2010.

[25] ——, "Tracking Rectangular and Elliptical Extended Targets Using Laser Measurements," in *Proceedings of the 14th International Conference on Information Fusion (Fusion 2011)*, Chicago, Illinois, USA, Jul. 2011.

[26] K. Granström and U. Orguner, "A PHD Filter for Tracking Multiple Extended Targets Using Random Matrices," *IEEE Transactions on Signal Processing*, vol. 60, no. 11, pp. 5657–5671, Nov. 2012.

[27] S. J. Julier and J. K. Uhlmann, "Unscented Filtering and Nonlinear Estimation," in *Proceedings of the IEEE*, vol. 92, no. 3, 2004, pp. 401–422.

[28] W. Koch, "Bayesian Approach to Extended Object and Cluster Tracking using Random Matrices," *IEEE Transactions on Aerospace and Electronic Systems*, vol. 44, no. 3, pp. 1042–1059, Jul. 2008.

[29] W. Koch and R. Saul, "A Bayesian Approach to Extended Object Tracking and Tracking of Loosely Structured Target Groups," in *Proceedings of the 8th International Conference on Information Fusion (Fusion 2005)*, vol. 1, Philadelphia, USA, Jul. 2005.

[30] J. Lan and X. R. Li, "Nonlinear Estimation by LMMSE-Based Estimation With Optimized Uncorrelated Augmentation," *IEEE Transactions on Signal Processing*, vol. 63, no. 16, pp. 4270–4283, Aug 2015.

[31] Y. Liu and X. R. Li, "Generalized Linear Minimum Mean-Square Error Estimation," in *Information Fusion (FUSION), 2013 16th International Conference on*, July 2013, pp. 1819–1826.

[32] L. Mihaylova, A. Carmi, F. Septier, A. Gning, S. Pang, and S. Godsill, "Overview of Bayesian sequential Monte Carlo methods for group and extended object tracking," *Digital Signal Processing*, vol. 25, no. 0, pp. 1–16, Feb. 2014.

[33] A. Milan, K. Schindler, and S. Roth, "Challenges of ground truth evaluation of multi-target tracking," in *Proc. of the CVPR 2013 Workshop on Ground Truth - What is a good dataset?*, Portland, Oregon, USA, Jun. 2013.

[34] J. Nascimento and J. Marques, "Performance evaluation of object detection algorithms for video surveillance," vol. 8, no. 4, pp. 761–773, Aug. 2006.

[35] N. Petrov, A. Gning, L. Mihaylova, and D. Angelova, "Box Particle Filtering for Extended Object Tracking," in *Proceedings of the 15th International Conference on Information Fusion (Fusion 2012)*. Singapore: IEEE, Jul. 2012, pp. 82–89.

[36] N. Petrov, L. Mihaylova, A. Gning, and D. Angelova, "A Novel Sequential Monte Carlo Approach for Extended Object Tracking Based on Border Parameterisation," in *Proceedings of the 14th International Conference on Information Fusion (Fusion 2011)*, Chicago, Illinois, USA, Jul. 2011.

[37] ——, "Group Object Tracking with a Sequential Monte Carlo Method Based on a Parameterised Likelihood Function," *Monte Carlo Methods and Applications*, 2012.

[38] M. Roth and F. Gustafsson, "An Efficient Implementation of the Second Order Extended Kalman Filter," in *Proceedings of the 14th International Conference on Information Fusion (Fusion 2011)*, Chicago, Illinois, USA,

July 2011.
[39] D. Schuhmacher, B.-T. Vo, and B.-N. Vo, "A Consistent Metric for Performance Evaluation of Multi-Object Filters," *IEEE Transactions on Signal Processing*, vol. 56, no. 8, pp. 3447 –3457, Aug. 2008.
[40] M. Wüthrich, S. Trimpe, D. Kappler, and S. Schaal, "A New Perspective and Extension of the Gaussian Filter," in *Robotics: Science and Systems*, 2015.
[41] C. L. Zitnick and P. Dollár, "Edge boxes: Locating object proposals from edges," in *The 10th European Conference on Computer Vision (ECCV 2008)*, Marseille, France, Oct. 2008.